Stiffness of dowel-type timber connections under pre-yield oscillating loads

Thomas Reynolds[a,*], Richard Harris[a], Wen-Shao Chang[a]

[a]*BRE Centre for Innovative Construction Materials, Department of Architecture and Civil Engineering, University of Bath, Claverton Down, Bath, BA2 7AY, UK*

Abstract

The dynamic behaviour of timber structures in service is becoming a more important consideration in design as modern engineered wood products allow longer spans and taller timber buildings, which can be sensitive to dynamic loading such as that from wind or footfall. Connections in timber structures have a pronounced effect on their structural behaviour. In dowel-type connections, the fasteners bend under load and embed into the surrounding timber and, since embedment is a nonlinear process, the stiffness of those connections varies depending on the nature of the applied load. Here, single-dowel connections are tested under cyclic loads representative of in-service vibration. One-sided and reversed cyclic loads are applied. The specimen stiffness is observed to reduce with the amplitude of one-sided cyclic load. For small-amplitude one-sided load, the specimen stiffness is seen to tend towards that predicted by an elastic model, and an analytical elastic model is presented to represent the embedment resistance of the timber and the behaviour of the connector.

Keywords: timber, connection, dowel, dynamic, vibration, serviceability

*Corresponding author

Email address: tpsreynolds@gmail.com (Thomas Reynolds)

1. Introduction

Dowel-type connections make a significant contribution to the stiffness of timber structures in which they are used, and most timber structures employ dowel-type connections in the form of either nails, screws, bolts or plain dowels. In recent years, engineered wood products such as glued-laminated and cross-laminated timber have allowed timber to be used in more ambitious structures, such as long-span bridge structures and multi-storey buildings, by allowing large member and panel sizes not possible in sawn timber. Such structures require thorough design for serviceability conditions, including vibration under dynamic loads such as wind and footfall.

The behaviour of dowel-type connections includes nonlinear and irreversible components, even under loads well below their nominal yield load. For example, the stiffness exhibited when a load is first applied is different to that when the load is removed and reapplied. Therefore, if the connection stiffness is to be represented by an equivalent linear elastic stiffness, as is the case in most structural engineering analysis, then that stiffness must be chosen to be appropriate to the nature of the applied load. This study investigates the stiffness of dowel-type connections under the cyclic loads resulting from in-service structural vibration, and presents an analytical model based on the elastic material properties of the timber and connector, which is shown to predict the underlying elastic response on which the nonlinear behaviour is superimposed.

The nonlinear stiffness under in-service loads differs from that under seismic loads, which have been widely studied and in which gross plastic behaviour occurs in timber and connectors. This research therefore extends

the field by providing empirical evidence of the stiffness and energy dissipation in dowel-type connections under in-service dynamic loads, and the basis of a predictive model for their stiffness in those conditions.

2. Background

There has been a great deal of research into the dynamic performance of timber structures with dowel-type connections under the forces and displacements associated with seismic loading, measuring stiffness, and its variation of with the amplitude and duration of the applied cyclic load [1, 2, 3, 4, 5, 6]. There has been far less research into the stiffness of connections under the pre-yield loads associated with in-service loading by dynamic forces such as wind and footfall.

Chui and Ni [7] carried out cyclic tests on connections with gradually increasing amplitude of load, and observed the development of hysteresis loops. A lower-stiffness region at low load was observed to occur as a result of local plastic behaviour around the dowel. This behaviour had been widely noted, but not thoroughly investigated until the study by Dorn et al. [8], who attributed it to the contact stiffness between the imperfect surface of the timber, and the relatively smooth and hard surface of the steel. Dorn et al. studied serviceability loads, but focussed primarily on monotonic, rather than cyclic loading.

This study adds to the current knowledge of the vibration behaviour of timber structures by measuring the stiffness in complete connections under one-sided and reversed loads representative of in-service vibration. An analytical model is then applied to asses the underlying elastic stiffness of the

connections onto which the nonlinear behaviour, considered to be due to the interaction between dowel and timber at the contact surface, is superimposed.

The connection is modelled as a beam, representing the steel dowel, on a foundation representing the embedment resistance of the timber. The beam-on-foundation model was first applied to timber connections by Kuenzi [9], and beam on foundation models were later used to model nailed connections, using non-linear embedment parameters for timber and connector [10, 11, 12].

The stress-strain behaviour of steel can be readily used to evaluate the behaviour of the beam in its elastic and plastic ranges. The foundation modulus, in contrast, has conventionally been empirically defined [7, 13, 14]. Embedment has also been modelled using the finite element method [15, 16]. A model for embedment must take into account the contact behaviour and friction at the interface between dowel and timber. Finite-element models therefore must include contact elements, which adds to their computational intensity.

This study sought to define and test an analytical model for embedment and connection stiffness. Such a model must represent the behaviour of an orthotropic elastic material, the timber, around a hole loaded by frictional contact with a rigid circular section, the dowel. This situation is generally referred to as a pin-loaded plate, and is common to timber and fibre-reinforced composite structures. A general analytical solution was defined by Lekhnitskii [17], and was developed by other researchers for analysis of the stress distribution around the hole [18, 19, 20, 21]. Reynolds et al. [22] extended the application of the method to prediction of displacements, and applied the solution by Zhang and Ueng [21] to estimate the stiffness measured in cyclic

embedment tests on half-hole embedment specimens according to ASTM D5764 [23].

In this study, the analytical stress function defined by Hyer and Klang [20] is used and extended to predict the stiffness of complete simplified connections. The model is compared with experimental results for cyclic loads representative of in-service vibration.

3. Materials and Methods

The experimental work in this study used Norway spruce (Picea abies) glued-laminated timber (glulam), delivered with a cross-section of 190mm by 200mm, made up of five 40mm laminates. The glulam was strength-graded as GL28h according to EN 1194 [24]. After delivery, its moisture content was measured by electrical resistance to be 11.3%. The specimens were cut from the glulam and stored in a controlled environment at 18-22°C and 60-65% relative humidity for a period of 7 months, which was assumed to be sufficient for equilibrium moisture content to be achieved. After testing, 7 specimens were cut from the single-dowel connection test specimens for evaluation of this equilibrium moisture content according to EN 13183 [25]. The moisture content had a mean of 11.9% with a coefficient of variation of 0.05. The density of the glulam was measured as 458kg/m^3, which could be corrected to give 461kg/m^3 at 12% moisture content. This is 12% higher than the 410kg/m^3 for standard GL28h.

The nominally 12mm dowels were specified by the supplier as C16 bright steel according to EN 10277 Part 2 [26]. The dowels were measured as having a diameter of 11.8mm, and the holes in the timber were predrilled using a

12mm auger drill bit. The steel plates were 6mm thick, and inserted into a 7mm slot in the timber piece.

Specimens were rejected if they contained a substantial visible defect in the surface of the timber within 25mm of the holes for the connectors. Otherwise, the specimens were used as delivered, incorporating defects elsewhere in the timber.

3.1. Single-dowel connection test

The single-dowel connection test was intended to investigate the processes which contribute to stiffness in a connection in which the dowel transmits force from the timber to a steel plate in a central slot. Loads in tension and compression were applied to each specimen to investigate the effect of the different stress distributions in the timber on stiffness. The specimen was made symmetrical, with a connection at each end, which removed the need to anchor the specimen, since a stiff anchorage could not be readily achieved in tension. Only the movement of the loading head was measured, so the measured deformation represented the sum of the deformations in the two connections. The movement of the loading head was measured using a $\pm$1mm LVDT on an adjustable steel mounting. The moving rod of the LVDT was attached to the loading head adjacent to the jaws in which the steel plates were clamped, and the fixed part of the LVDT was attached to a steel mounting attached to the test bed. In the tests with fully reversed loading, the displacements were out of the range of the LVDT, and so the internal displacement sensor in the loading machine was used. The LVDT which was used had no connection between the moving rod and the fixed body, the rod moved freely through the coil, and was attached by a magnet to the loading

head. This ensured that no force was transferred to the mounting of the LVDT, so that there would be no movement of the LVDT body during the test. This was crucial given the small differential movements, of the order of microns, which were to be measured. It was assumed that the steel plates did not slip in the jaws of the loading machine, and that their deformation was negligible in comparison with the deformation in the connections.

BS EN 383 [27] gives recommended dimensions for a symmetrical static embedment test specimen parallel-to-grain, and so these dimensions were used to aid comparisons with work by other researchers. No guidance is given in EN 383 [27] for tests in tension perpendicular-to-grain, so the specimen dimensions were determined to match the compression tests in that standard, with the distance between the dowels specified to be double that between the dowel and the test bed in the standard. The thickness of the specimens was chosen as 190mm, so that the failure loads for one and three plastic hinges were close for both parallel and perpendicular to grain, according to Eurocode 5 [28]. Although the loads applied were well below those necessary for any plastic hinges to form, this was considered to represent a common situation, since it is recommended that connections are designed to form one or three plastic hinges to ensure ductility. The specimens are shown schematically in Figure 1.

The embedment strength of the timber was calculated based on the density of 461kg/m^3, according to Eurocode 5 [28]. This gave an embedment strength of 33N/mm^2 parallel to grain and 22N/mm^2 perpendicular. These embedment strengths were used to calculate the expected connection strengths of 14.2kN parallel, and 11.7kN perpendicular.

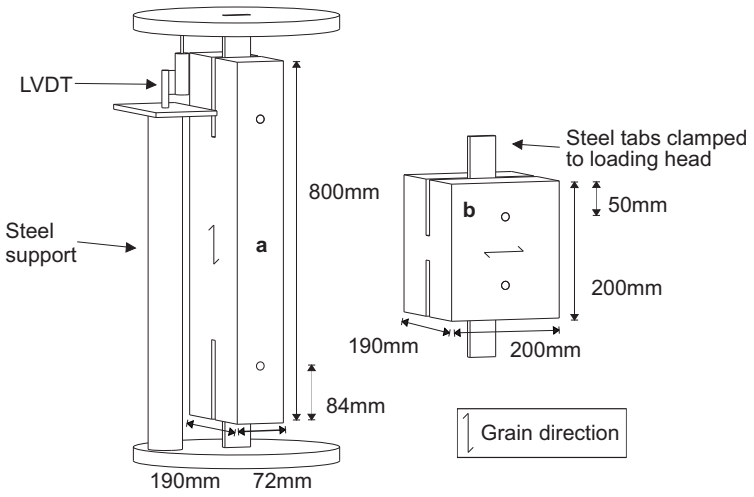

Figure 1: Test setup and specimen dimensions for single-dowel connection tests **a** parallel to grain and **b** perpendicular to grain

3.2. Loading

The magnitude and form of oscillating load was chosen to be a simplified representation of the different forms of load which could result from in-service vibration. Since problematic vibration is commonly a result of resonance, such loads can be expected to have a dominant sinusoidal component [29, 30]. A sinusoidal variation of displacement was therefore applied, the mean and amplitude of which was defined by the R-ratio, given by $R = F_{max}/F_{min}$ where F_{max} is the maximum load in the compressive sense and F_{min} the minimum. R-ratios of 1.2, 10 and -1 were used.

R=1.2 and R=10 represent different ratios between the extremes of force in a one-sided oscillating load. One-sided loading occurs, for example, in vertical footfall-induced vibration, in which the mean load applied by the self-weight of the structure is larger than the dynamic load applied by footfall, so that the load on the structure is never reversed. One-sided loading also occurs

in along-wind vibration of structures, in which the mean wind force is larger than the dynamic component caused by turbulence. R=-1 represents fully-reversed loading, which occurs in across-wind vibration or lateral footfall-induced vibration in which the mean load is zero.

The frequency of the oscillating load was 1Hz, chosen to be within the range of vertical and lateral structural vibration. Vertical footfall-induced vibration generally occurs at frequencies higher than 1Hz, and the lateral mode natural frequency of tall buildings can be lower, but 1Hz was considered to be a reasonable frequency to investigate the general principles of behaviour under oscillating load in this range. The magnitude of the oscillating load was characterized by the peak value, and the tests used peak loads of 20% and 40% of the characteristic yield load of the connection according to Eurocode 5 [28]. These levels of load are considered to be approximately representative of the range of load imposed on a structural component during everyday use of a structure.

The duration of cyclic loading was chosen to ensure that any transient effects could be observed and that a single value of either stiffness or energy dissipation could be measured which was representative of the long-term steady-state behaviour. The load was applied for 1000 cycles, which proved sufficient for the stiffness and energy dissipation to reach a representative steady state. The tests were carried out in displacement control, since it was found that the nonlinearity in the response caused the servo-hydraulic loading machine to become unstable in load control. The displacements for the peak and trough of the cyclic loads were determined at the start of the test.

The sequence of single-dowel connection tests is shown in Table 1. Each specimen was tested for each load level, R-ratio and load direction. Three specimens were tested for each grain orientation, six specimens in total. The tests with lower peak loads were carried out first, so that each test represented the highest load the specimen had seen, and tests with R=1.2 were carried out before those with R=10, with the R=-1 test last of all. Since the purpose of this study was to measure steady-state behaviour after repeated cycles of load, it was considered that the previous loading at the same or lower load level would not have a significant effect on the measured stiffness and energy dissipation, though it is expected that the previous loading may cause the specimen to reach the steady-state more quickly.

3.3. Friction test

In addition to the elastic material properties for the timber, the elastic stress-function model presented in Section 5 required the friction coefficient between the dowel and the surrounding timber. This was estimated using the test setup shown schematically in Figure 2. The friction coefficient between dowel and timber was estimated based on the ratio between the force applied to the dowel to produce continuous movement and the normal force applied to the specimens, which was either 20% or 40% of their predicted embedment strength given in Section 3.1. Six specimens were tested, three parallel to grain and three perpendicular, and their dimensions are shown in Figure 2. The specimens were taken from the same batch of Norway spruce glulam used for the single-dowel connection tests. As in the case of the single-dowel connection specimens, the holes were drilled using a pillar drill and an auger bit, and the bright mild steel dowel was cleaned and de-greased before testing.

Table 1: Single-dowel connection tests

Grain orientation	Load sequence	Load direction	Peak load		R-Ratio
			% of yield	kN	
Parallel	1)	Compression	20%	2.84	1.2
	2)		20%	2.84	10
	3)		40%	5.68	1.2
	4)		40%	5.68	10
	5)	Tension	20%	2.84	1.2
	6)		20%	2.84	10
	7)		40%	5.68	1.2
	8)		40%	5.68	10
	9)	Reversed	40%	5.68	-1
Perpendicular	1)	Compression	20%	2.34	1.2
	2)		20%	2.34	10
	3)		40%	4.68	1.2
	4)		40%	4.68	10
	5)	Tension	20%	2.34	1.2
	6)		20%	2.34	10
	7)		40%	4.68	1.2
	8)		40%	4.68	10
	9)	Reversed	40%	4.68	-1

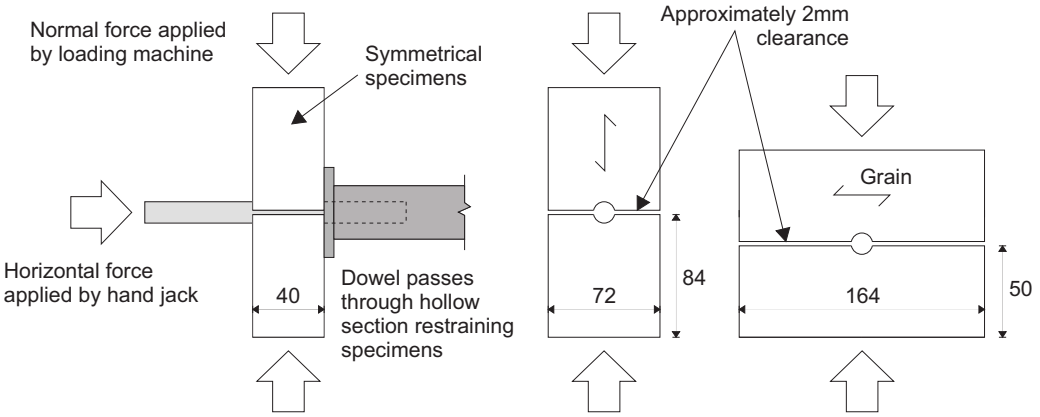

Figure 2: Schematic diagram of friction test setup

It was noted that the orientation of the friction force in this test was different to the orientation of the friction around the dowel as it embeds into the surrounding timber. Nonetheless, this test was considered to provide a reasonable estimate of the coefficient of friction, given that a more extensive study of friction between steel and timber by McKenzie and Karpovich [31] showed little variation of friction coefficient with angle to grain.

4. Experimental Results and Discussion

Under its first loading, the gradual compression of the contact surface between dowel and timber, as well as viscoelastic behaviour in the timber itself, lead to a transient variation in stiffness. These effects were observed by calculating the secant stiffness for every cycle of applied load during the test.

Figure 3 shows the force-displacement plots for a single cycle at each of the three R-ratios on the same parallel-to-grain specimen. The 100th and 900th cycles are shown in each case. Figure 3 also indicates how the secant

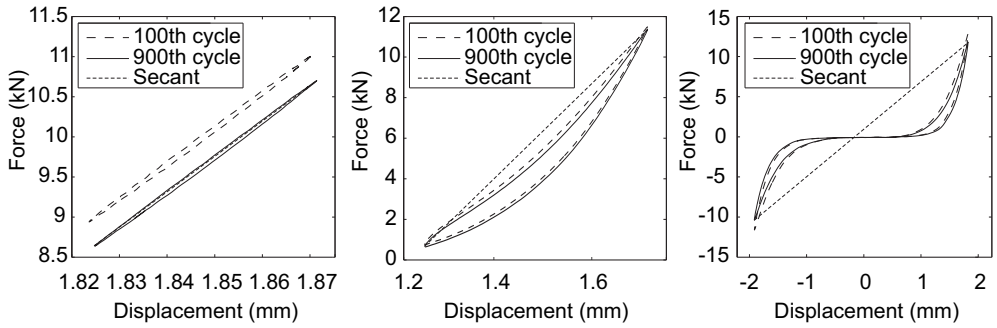

Figure 3: Force-displacement plots for parallel-to-grain tests in compression with R=1.2, left, R=10, centre, and R=-1, right - the gradient of the dotted line is the secant stiffness for the 900th cycle in each case

stiffness was calculated in each case.

The slack section in the R=-1 plot, where the loading head moves with very little force applied, is due both to the clearance between the dowel and the holes in the steel plates that load the specimen and the gap formed by irreversible behaviour in the surface of the timber. The dowels, nominally 12mm, were measured as having a diameter of 11.8mm, and the holes in the steel plate were drilled to 12.5mm. The total slack due to this clearance in each of the two dowels was therefore approximately 1.4mm, and so accounts for a significant proportion of the displacement at near-zero force shown in the R=-1 plot in Figure 3.

The results shown in Figure 3 are for parallel-to-grain tests in compression. The other grain and load orientations show qualitatively the same behaviour: at R=1.2 the force-displacement behaviour is close to linear with a small area inside the hysteretic loop in comparison with R=10, at which more non-linearity is apparent, and at R=-1 gap formation is seen to influence the force-displacement response.

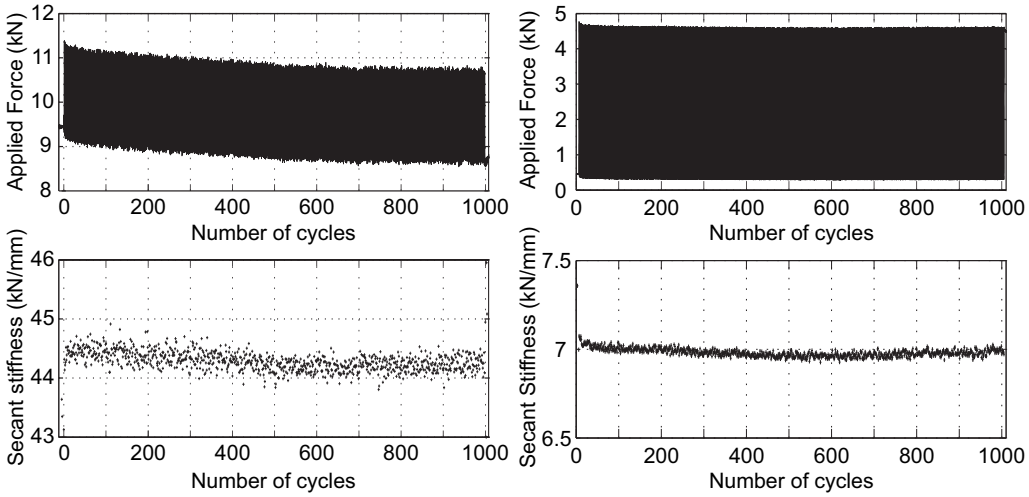

Figure 4: Stiffness in each cycle of load through the test, for a specimen loaded in compression parallel to grain to 40% of its characteristic yield load, with an R-ratio of 1.2 (left hand plots) and in tension perpendicular to grain to 20% of its characteristic yield load, with an R-ratio of 10 (right hand plots).

The graphs in Figure 4 show the variation of secant stiffness through a 1000-cycle test. In both the tests shown, the stiffness tends towards an approximately constant value during the test, after variation in the first 500 to 700 cycles. In some tests, there was still evidence of variation in stiffness after 1000 cycles. In those cases, the measured stiffness may differ slightly from the steady-state value. It is acknowledged that there may be longer-term effects which are not apparent in the duration of these tests. The scatter of stiffness is considered to be primarily due to measurement noise, and there is far less scatter in the tests at R=10 due to the larger differential displacements and forces being measured.

It can be seen from Figure 4 that, since the test is carried out in displacement control, the force applied to the specimen reduces with time due

to viscoelastic behaviour in the timber. This results in the shift in the force-displacement diagram between the 100th and 900th cycles in Figure 3. This shift only affects the secant stiffness in the case of the fully-reversed load with R=-1, since it represents a gap formation in the connection, and the gap is not crossed in one-sided loading.

In the other grain and load orientations same qualitative behaviour was observed: a tendency of stiffness towards a relatively consistent value over the course of the test. The quantitative differences between the specimens are presented in Figure 5.

Figure 5 shows the secant stiffness measured in the single-dowel tests with R=10, R=-1 and R=1.2. The secant stiffness is expressed as the mean value over the final 300 cycles in the test. This was taken to be a reasonable estimate of the steady-state values.

More scatter can be seen in the measured stiffness in the perpendicular-to-grain tests than in the parallel-to-grain tests. In the parallel-to-grain tests, the stiffness, plotted in Figure 5, is observed to increase slightly with the peak value of the applied load. It is considered that the increase in stiffness is due to the higher applied force compressing the surface of the timber and improving the stiffness of the contact between dowel and timber. This suggests that as the contact between the dowel and timber improves, the stiffness of the connection tends towards a value which represents a rigid contact surface. This concept is important in considering how the connection is modelled in Section 5, since it suggests that, to predict the steady-state stiffness and energy dissipation in the connector, a model with a rigid contact surface may be appropriate.

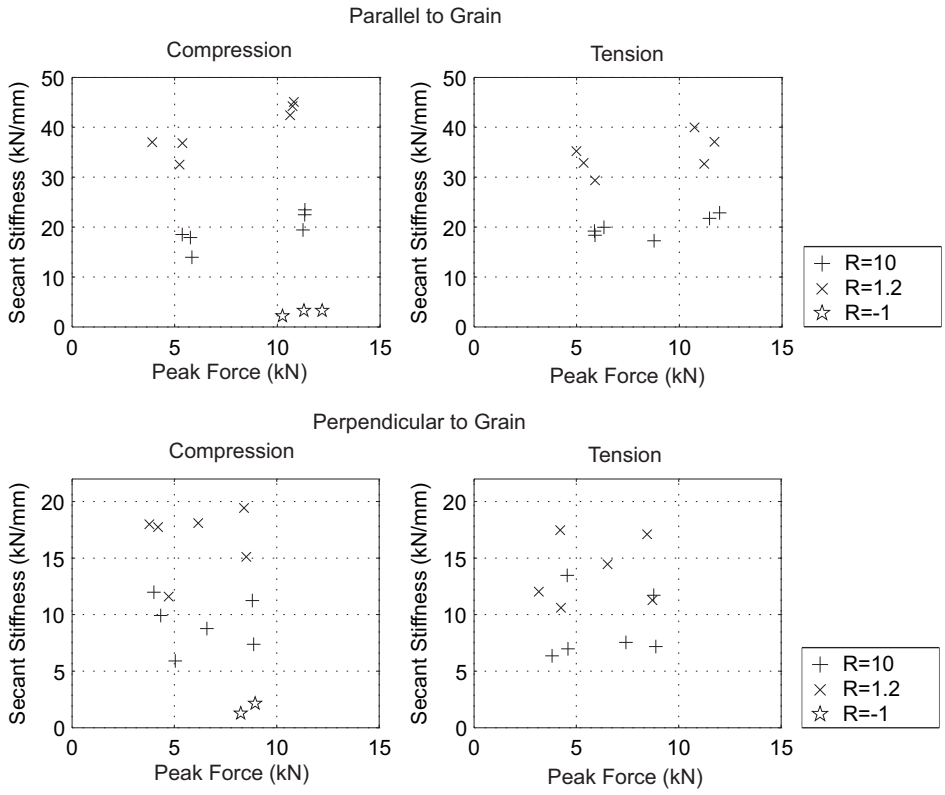

Figure 5: Secant stiffness for single-dowel connection tests

The perpendicular-to-grain tests in Figure 5 do not show the same tendency for an increase in stiffness with the peak value of the applied load. In the perpendicular-to-grain direction, therefore, it appears that the plastic processes in the contact surface are largely complete at 20% of the characteristic yield load, and have little further effect at higher loads.

Student's t-test [33] was applied to estimate the likelihood that the observed variation in stiffness with the magnitude of the peak load was a result of experimental scatter. The test was developed for analysis of small samples such as the three repetitions in these tests, and returns a probability that a

Table 2: Student's t-test applied to investigate the effect of variation in peak load on the secant stiffness measured in single-dowel connection tests: $\overline{d}$ mean of the difference in stiffness at each peak load, s_x is the standard deviation of those differences, n is the number of specimens, ν is the number of degrees of freedom for the t-distribution, t is the test statistic and p the probability that the null hypothesis is true

	$\overline{d}$	s_x	n	ν	t	p
Tension						
Perpendicular	0.91	1.42	3	2	1.11	0.38
Parallel	4.11	0.73	3	2	9.70	0.01
Compression						
Perpendicular	1.60	1.46	3	2	1.90	0.20
Parallel	8.46	1.33	3	2	10.99	0.01

null hypothesis, that both samples are taken from populations with the same mean, is true. Since tests with different peak loads were carried out on each specimen, a paired-variable t-test was used. The application to the parallel to grain tests shown in Table 2 therefore returns the probability p that the change in peak load from 20% to 40% of the characteristic yield load has no influence on the secant stiffness.

The results show that, in the parallel-to-grain tests, it is extremely likely that there is an influence of peak load on stiffness, with probabilities of 0.01 in each case that the null hypothesis is true. The influence of peak load in the perpendicular-to-grain tests is less clear, as shown in the table.

The Eurocode 5 slip modulus represents current design guidance to cal-

culate the stiffness of a connection [28]. Applying that guidance to this specimen results in a predicted stiffness of 10.2kN/mm, without including the slip due to the oversize of the hole in the steel plate. That guidance makes no allowance for grain direction, and can be seen to be a significant underestimate for the parallel-to-grain tests, especially with R=1.2, where the underestimate is by as much as a factor of 4. The Eurocode slip modulus is intended for calculation of deflections under static loads, rather than such small-amplitude oscillating load, and this is considered to be the reason for this discrepancy. The result therefore highlights the importance of the nature of the applied load to the stiffness of this type of connection.

Figure 5 shows that the measured secant stiffnesses under R=1.2 loads are generally higher than those with R=10. Since each specimen was tested at each amplitude, it was possible to analyse these results as paired variables. The ratio of the stiffness at R=10 to that at R=1.2 was compared for every load level and every specimen, and the results are shown in Figure 6. It can be seen that in every case, the stiffness measured at R=10 is lower than that at R=1.2, and that the ratio is in a relatively concentrated range, with a mean value of 0.56 for all the tests. An independent-variable t-test comparing the parallel- and perpendicular-to-grain ratios shows that it is likely there is an influence of grain direction, with a probability of 0.06 that that two samples come from populations with the same mean. The mean ratio of the R=-1 secant stiffness to that at R=1.2 is 0.07 in the parallel-to-grain orientation and 0.12 perpendicular to grain.

The reduced stiffness at R=-1 includes the slip due to the oversize of the holes in the steel plates. If the deflection, estimated as 1.4mm, due to this

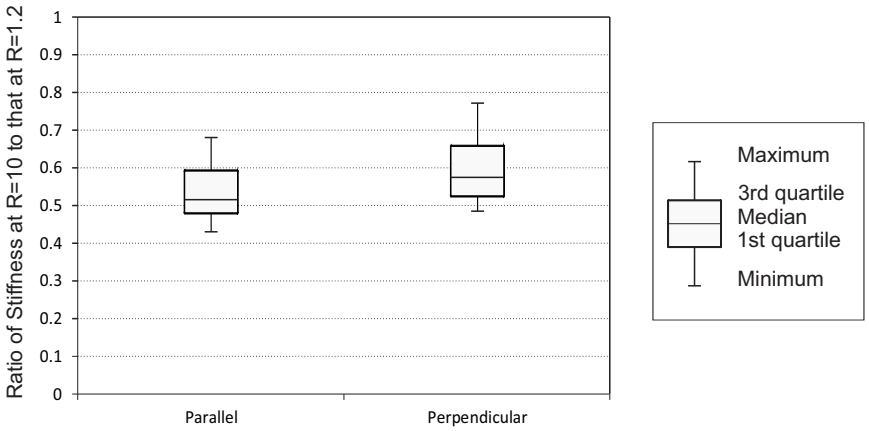

Figure 6: Box plot for reduction in stiffness between R=1.2 and R=10 for the collated results of tests in tension and compression, at 20% and 40% of the characteristic yield load

oversize is excluded, then the mean ratio of the R=-1 secant stiffness to that at R=1.2 is 0.12 parallel to grain and 0.17 perpendicular. The reduction in stiffness between R=1.2 and the reversed load with R=-1 is due to a combination of the low stiffness for low load in embedment, gap formation in the timber and the oversize of the hole in the steel plate. Some of this gap formation will have occurred in viscoelastic behaviour during the one-sided tests at R=1.2 and R=10, which were carried out before the reversed R=-1 tests. In this sense, the secant stiffness for the R=-1 tests presented here is related to the particular loading history applied to the specimens, in a way that is not the case for the one-sided tests, in which the viscoelastic behaviour is considered to significantly affect the overall displacement, but not the secant stiffness.

5. Model

5.1. Foundation modulus

Reynolds et al. [22] showed that the stiffness of the embedment test could be modelled analytically by superposition of stress functions for a pin-loaded half-hole in a semi-infinite orthotropic plate. This study uses a different version of the stress function to Reynolds et al. [22], one proposed by Hyer and Klang [20], which represents the stress field around a complete hole in a pin-loaded orthotropic plate, in order to model the behaviour of a complete connection.

Hyer and Klang used the stress function to calculate the stresses around the hole edge. It has been shown that such a stress function can be used to calculate the field of displacements in the timber around the dowel, and so the movement of the dowel relative to a particular fixed point [22]. The stress function is two dimensional for the plane-stress condition and thus, when used to calculate the embedment stiffness of the timber around the dowel, gives the stiffness of a unit thickness of material along the dowel. It also, therefore, does not allow for some effects of the full elastic foundation provided by the timber, such as the effect of non-uniform loading along the dowel's length.

The solution by Hyer and Klang [20] was slightly modified by adding the term in p, the mean stress in the member, as proposed by Echavarría et al. [19] to account for the finite extent of the loaded member. The resulting equation for the stress functions $\phi_{1,2}$ is given in (1) and (2). The transformed coordinates $\zeta_{1,2}$, the roots of the characteristic equation $\mu_{1,2}$ and the coefficients a_n and b_n representing the load on the hole edge are all as defined

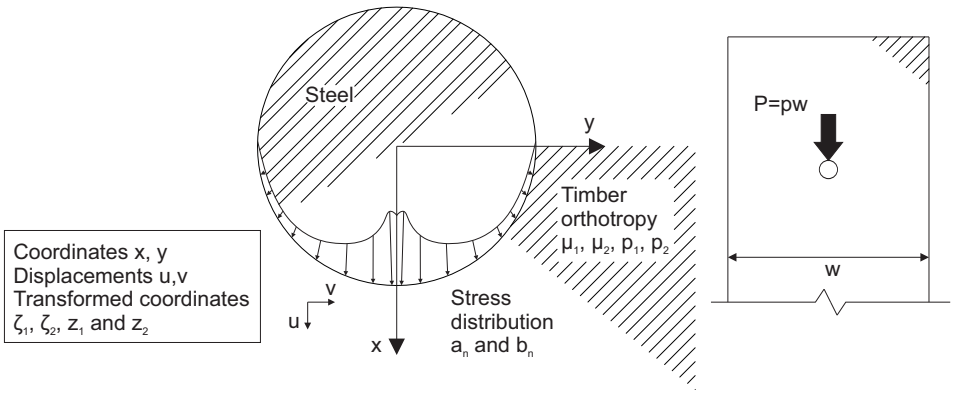

Figure 7: Illustration showing notation for the stress function model for embedment

by Hyer and Klang [20] and Lekhnitskii [17], and the solution follows Hyer and Klang's method. The effect of friction is to alter the distribution of load around the hole edge, and is therefore reflected in the coefficients a_n and b_n, which are calculated by an iterative process [20]. The notation is illustrated in Figure 7.

$$\phi_1 = a_0 \ln \zeta_1 + \frac{p}{2}\left(\left(\frac{-i}{\mu_1 - \mu_2}\right)\frac{1}{\zeta_1} + \frac{z_1}{\mu_1^2 - \mu_2^2}\right) + \sum_{n=1}^{\infty}\frac{a_n}{\zeta_1^n} \tag{1}$$

$$\phi_2 = b_0 \ln \zeta_2 + \frac{p}{2}\left(\left(\frac{-i}{\mu_2 - \mu_1}\right)\frac{1}{\zeta_2} + \frac{z_2}{\mu_2^2 - \mu_1^2}\right) + \sum_{n=1}^{\infty}\frac{b_n}{\zeta_2^n} \tag{2}$$

The displacements in the loaded direction u can then be calculated according to 3 [17], where p_1 and p_2 are calculated from the material properties, as given by Lekhnitskii [17].

$$u = 2\mathrm{Re}\left(p_1\Phi_1 + p_2\Phi_2\right) \tag{3}$$

Figure 8 shows the result of superimposing two stress functions with loads in opposite directions to give the field of deformation in the specimen. The

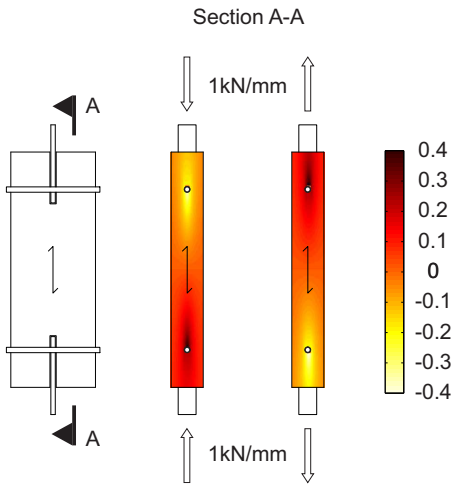

Figure 8: Field of vertical displacement in mm in the timber under a dowel load of 1kN per mm thickness, used to calculate the foundation modulus for the connection

displacement of each dowel relative to the line of zero displacement mid way between the dowels is then used to calculate a foundation modulus for the single-dowel connection tests. As shown by Hyer and Klang [20], if the dowel fits tightly into the hole, the relationship between force and dowel displacement is linear, so the foundation modulus is constant with dowel displacement.

It should be noted that, in contrast to current methods for assessment of the foundation modulus, this model takes into account the distance between connectors. This includes both by the elastic deformation of the timber between the dowels under the mean stress, which would normally be accounted for elsewhere in the analysis, and the effect of the stress concentration which gradually equalizes along the length of the member.

5.2. Beam on foundation

The stress function allows for the embedment behaviour of the dowel in the timber. In the single-dowel connection tests, there is deformation of the dowel, and this is represented by a beam-on-foundation model, in which the resistance of the timber to embedment is represented by a foundation modulus, and the dowel by a beam to which the appropriate loads are applied. Since the steady-state cyclic embedment behaviour under the smaller-amplitude R=1.2 loads appears to be close to linear-elastic, the foundation provided by the timber was considered as elastic for that form of load. The model is not intended to represent the reduced stiffnesses at R=10 and R=-1 which have been treated empirically in this study.

For the connections with a central flitch plate used in this study, the deflection which defines the connection stiffness is at the centre of the beam, where the load is applied. The beam is of finite length, equal to the length of the dowel, and the reaction at the foundation is proportional to its displacement: a Winkler foundation [34]. A widely-used analytical solution exists for this geometry of a beam on elastic foundation, and is used in this study [35].

5.3. Comparison with experiment

The model was used with the material properties shown in Table 3. Since the timber was graded and the moisture content was within 1.5% of the standard 12% value for all of the specimens, it was considered appropriate to use the material properties given for glulam in EN 1194 [24]. That standard does not provide the Poisson's ratio, so that value was taken as given by Bodig and Jayne [36] for Spruce. The friction test described in Section 3.3

Table 3: Material properties used in connection stiffness calculation, taken from (1) EN 1194 [24], (2) Bodig and Jayne [36] and (3) friction tests

Elastic moduli (1)		Shear Modulus (1)	Poisson's ratio (2)	Coefficient of friction (3)
N/mm^2	N/mm^2	N/mm^2		
12600	420	780	0.422	0.176

gave a mean kinetic friction coefficient of 0.168 for the six tests, with a coefficient of variation of 0.15, and a mean static friction coefficient of 0.184 with a coefficient of variation of 0.11. It was considered that both the static and kinetic friction cases would be relevant during the tests, since some parts of the interface between dowel and timber would be moving relative to one another, and some would not. The mean of the two values was therefore used in the model. The influence of the friction coefficient on the predicted stiffness was found to be small in this range: the stiffness predicted using the static friction coefficient was, as a maximum for the grain and load orientations, 0.5% higher than that using the kinetic coefficient. The assumption of a single friction coefficient, taken as the mean of the two values, was therefore considered appropriate.

Table 4 shows the predicted stiffness of the embedment and single-dowel connection specimens compared with the measured stiffness in the tests with R=1.2. The results show that the measured stiffness under cyclic load is lower than the elastic stiffness in most of the tests, with the exception of the perpendicular-to-grain single-dowel tests.

The reason that the elastic model generally over-predicts the stiffness

Table 4: Comparison of predicted elastic stiffness with the secant stiffness measured in cyclic load tests with R=1.2

Grain orientation	Load direction	Predicted elastic	Measured stiffness	
			Mean	Standard deviation
		kN/mm	kN/mm	kN/mm
Parallel to grain	Compression	41.9	39.7	5.0
Perpendicular to grain	Compression	14.5	16.7	3.7
Parallel to grain	Tension	39.7	34.5	2.9
Perpendicular to grain	Tension	13.4	13.8	3.0

is considered to be that it does not account for the effect of the imperfect contact surface between dowel and timber. The model assumes that the load is transferred between dowel and timber through a perfectly rigid contact. In the experiments, the surface of the timber in contact with the dowel is uneven, as a result of the drilling process, and this unevenness reduces the stiffness of the connection as a whole. The effect is most pronounced at low loads, so the R=10 cyclic tests, in which the load reduces to almost zero in each cycle, have a greater reduction in stiffness than the R=1.2 tests. The model is therefore only compared with the results of the R=1.2 tests.

The underprediction in the perpendicular-to-grain single-dowel connection tests is thought to be due to the fact that the Winkler foundation in the beam-on-elastic-foundation model does not allow for distribution of load by shear in the foundation, which may be especially prevalent perpendicular to grain, since the ratio of the shear modulus to the foundation stiffness is

higher than in the parallel-to-grain tests.

The fact that the measured density of the glulam was 12% higher than the standard density for GL28h according to EN1194 [24] means that the stiffness of the material might be expected to be slightly higher than modelled. This would have the effect of reducing, or perhaps eliminating, the underestimate in the perpendicular-to-grain tests, and increasing the overestimate parallel to grain.

6. Conclusion

It has been shown through experimental work that the stiffness exhibited by a dowel-type connection under cyclic load depends on the nature of the loads applied to it. The cyclic loads applied in this study were representative of in-service vibration of a structure, in that their peak value was well below the ultimate strength of the connection.

It was seen that the secant stiffness of the connection was highest under one-sided oscillating load in which the mean load was large compared with the cyclic component. In these conditions, the specimen stiffness was close to that predicted by an elastic analysis consisting of a stress function for embedment and a beam-on-elastic-foundation model for dowel bending. As the amplitude of the cyclic component was increased in comparison to the mean, the secant stiffness reduced, and the energy dissipation increased. Under reversed cyclic load, the oversize of the hole in the steel loading plate and gap formation in the timber led to further reduction in the secant stiffness. These trends were evident in both parallel- and perpendicular-to-grain specimens, though a greater scatter in stiffness was observed in the perpendicular-to-

grain specimens.

In its current form, the model could be applied to estimate connection stiffness for prediction of behaviour under small-amplitude one-sided dynamic loads similar to those applied in the R=1.2 tests. An example would be footfall-induced vibration of a footbridge, in which the dynamic force is small in comparison with the self-weight. Further work could extend the model to account for the reduction in stiffness resulting from nonlinear behaviour at low load, which would enable it to be applied to a wider range of dynamic in-service loads.

References

[1] Ceccotti, A.. New technologies for construction of medium-rise buildings in seismic regions: The XLAM case. Structural Engineering International 2008;18(2):156–165.

[2] Filiatrault, A., Christovasilis, I.P., Wanitkorkul, A., Lindt, J.W.v.d.. Experimental seismic response of a full-scale light-frame wood building. Journal of Structural Engineering 2010;136(3):246–254.

[3] Filiatrault, A., Isoda, H., Folz, B.. Hysteretic damping of wood framed buildings. Engineering Structures 2003;25(4):461–471.

[4] Folz, B., Filiatrault, A.. Cyclic analysis of wood shear walls. Journal of Structural Engineering 2001;127(4):433–441.

[5] Heiduschke, A.. Analysis of wood-composite laminated frames under dynamic loads - analytical models and model validation. part ii: Frame

model. Progress in Structural Engineering and Materials 2006;8(3):111–119.

[6] Polensek, A., Schimel, B.D.. Dynamic properties of light-frame wood subsystems. Journal of Structural Engineering 1991;117(4):1079–1095.

[7] Chui, Y., Ni, C.. Load-embedment response of timber to reversed cyclic load. Wood and Fiber Science 1997;29(2):148–160.

[8] Dorn, M., de Borst, K., Eberhardsteiner, J.. Experiments on dowel-type timber connections. Engineering Structures 2013;47(0):67–80.

[9] Kuenzi, E.W.. Theoretical design of a nailed or bolted joint under lateral load. Tech. Rep. D1951; US Department of Agriculture, Forest Service, Forest Products Laboratory; 1955.

[10] Chui, Y.H., Ni, C., Jiang, L.. Finite-element model for nailed wood joints under reversed cyclic load. Journal of Structural Engineering 1998;124(1):96–103.

[11] Foschi, R.. Modeling the hysteretic response of mechanical connections for wood structures. In: World Conference of Timber Engineering. Whistler, B.C., Canada; 2000,.

[12] Sawata, K., Yasumura, M.. Estimation of yield and ultimate strengths of bolted timber joints by nonlinear analysis and yield theory. Journal of Wood Science 2003;49(5):383–391.

[13] Foschi, R., Yao, F., Rogerson, D.. Determining embedment response

parameters from connector tests. In: World Conference on Timber engineering. Whistler, B.C., Canada; 2000,.

[14] Sawata, K., Yasumura, M.. Determination of embedding strength of wood for dowel-type fasteners. Journal of Wood Science 2002;48(2):138–146.

[15] Dorn, M.. Investigations on the serviceability limit state of dowel-type timber connections. Ph.D. thesis; Faculty of Civil Engineering; 2012.

[16] Santos, C.L., De Jesus, A.M.P., Morais, J.J.L., Lousada, J.L.P.C.. A comparison between the EN 383 and ASTM D5764 test methods for dowel-bearing strength assessment of wood: experimental and numerical investigations. Strain 2010;46(2):159–174.

[17] Lekhnitskii, S.G.. Anisotropic Plates. 2nd ed.; New York: Gordon and Breach; 1968.

[18] De Jong, T.. Stresses around pin-loaded holes in elastically orthotropic or isotropic plates. Journal of Composite Materials 1977;11(3):313.

[19] Echavarría, C., Haller, P., Salenikovich, A.. Analytical study of a pinloaded hole in elastic orthotropic plates. Composite Structures 2007;79(1):107–112.

[20] Hyer, M., Klang, E.. Contact stresses in pin-loaded orthotropic plates. International Journal of Solids and Structures 1985;21(9):957–975.

[21] Zhang, K.D., Ueng, C.E.. Stresses around a pin-loaded hole in orthotropic plates. Journal of Composite Materials 1984;18(5):432–446.

[22] Reynolds, T., Harris, R., Chang, W.S.. An analytical model for embedment stiffness of a dowel in timber under cyclic load. European Journal of Wood and Wood Products 2013;71(5):609–622.

[23] ASTM, . Standard test method for evaluating dowel-bearing strength of wood and wood-based products (reapproved 2002). Tech. Rep. D5764-97a; ASTM; 1997.

[24] BSI, . Timber structures - glued laminated timber. Tech. Rep. BS EN 1194:1999; BSI; 1999.

[25] BSI, . Moisture content of a piece of sawn timber. Tech. Rep. BS EN 13183:2002; BSI; 2002.

[26] BSI, . Bright steel products - technical delivery conditions. Tech. Rep. BS EN 10277-2:2008; BSI; 2008.

[27] BSI, . Timber structures. test methods. determination of embedment strength and foundation values for dowel type fasteners. Tech. Rep. BS EN 383:2007; BSI; 2007.

[28] BSI, . Eurocode 5 design of timber structures part 1-1: General - common rules and rules for buildings. Tech. Rep. BS EN 1995-1-1:2004+A1:2008; BSI; 2009.

[29] Davenport, A.G.. How can we simplify and generalize wind loads? Journal of Wind Engineering and Industrial Aerodynamics 1995;5455(0):657–669.

[30] Ingólfsson, E.T., Georgakis, C.T., Jnsson, J.. Pedestrian-induced lateral vibrations of footbridges: A literature review. Engineering Structures 2012;45(0):21–52.

[31] McKenzie, W.M., Karpovich, H.. The frictional behaviour of wood. Wood Science and Technology 1968;2(2):139–152.

[32] BSI, . Timber structures. test methods. cyclic testing of joints made with mechanical fasteners. Tech. Rep. BS EN 12512; BSI; 2001.

[33] Student, . The probable error of a mean. Biometrika 1908;6(1):1–25.

[34] Winkler, E.. Die Lehre von der Elasticitaet und Festigkeit mit besonderer Rcksicht auf ihre Anwendung in der Technik, für polytechnische Schulen, Bauakademien, Ingenieure, Maschinenbauer, Architekten, etc. Prague: H Dominicus; 1867.

[35] Pikey, W.D.. Formulas for Stress, Strain and Structural Matrices. 2nd ed.; Hoboken, New Jersey: John Wiley and Sons; 2005.

[36] Bodig, J., Jayne, B.. Mechanics of wood and wood composites. Malabar, FL, USA: Krieger Publishing Company; 1993.